Int J Adv Manuf Technol (2015) 80:1173–1180
DOI 10.1007/s00170-015-7125-z

ORIGINAL ARTICLE

Fabrication and performance of monolayer brazed CBN wheel for high-speed grinding of superalloy

Qilin Li[1] · **Jiuhua Xu**[2] · **Honghua Su**[2] · **Weining Lei**[1]

Received: 15 September 2014 / Accepted: 6 April 2015 / Published online: 15 April 2015

Abstract The monolayer brazed wheels, which have several advantages such as high bonding strength, high chip storage space, and uniform grit spacing, have drawn much attention in the grinding of different-to-machine materials. As pursuing for higher machining efficiency, special attention has been devoted to high-speed grinding. However, when the grinding wheel is fabricated by conventional brazing technology, the thermal deformation of the wheel is remarkable, and the accuracy of brazed wheel cannot meet the needs of high-speed grinding. To take the challenge of the unexpected wheel deformation after brazing, a new brazing technology, named continuous induction brazing, was proposed to fabricate monolayer brazed cubic boron nitride (CBN) wheel with diameter d_s=400 mm for high-speed grinding. The experiments and analysis revealed that chemical bonding between CBN grains and filler alloy was achieved. The maximum thermal deformation of the newly brazed wheel was less than 16 μm. High-speed grinding performance of the brazed CBN wheel for grinding of Inconel718 superalloy showed that the grinding wheel has good bonding strength. Moreover, a relatively satisfactory ground surface quality was achieved.

✉ Qilin Li
liqilin@jsut.edu.cn

[1] School of Mechanical Engineering, Jiangsu University of Technology, 213001 Changzhou City, China

[2] College of Mechanical and Electrical Engineering, Nanjing University of Aeronautics and Astronautics, 210016 Nanjing City, China

Keywords High-speed grinding · Continuous induction brazing · Thermal deformation · Brazed CBN grinding wheel · Inconel718 superalloy

1 Introduction

Superalloys are often used as the material for turbine blades and jet engines of airplanes that requires high performance at elevated temperature [1]. On the other hand, superalloys have low heat conductivity and high strength, which make it very difficult to obtain effective grinding processes with high accuracy. As known to us, cubic boron nitride (CBN) abrasive grains have excellent physical properties. Consequently, CBN grinding wheels are widely used for grinding of different-to-machine materials, such as titanium alloy and nickel superalloy [2, 3].

In recent decades, a new monolayer CBN wheel was performed by brazing technique, which builds a chemical bridge between the grains and wheel with the help of an active braze alloy [4]. Comparing to the conventional electroplated counterparts, the monolayer brazed wheels have several advantages such as high bonding strength, high chip storage space, high wheel sharpness, and long service time, and have broad application prospect in grinding industry [5]. For example, Pal et al. [6] developed a monolayer brazed CBN grinding wheel, and the experimental investigation demonstrated the brazed-type wheel could grind the bearing steel more effectively and economically with lesser grinding forces and without wheel loading over wide ranges of the grinding parameters. They pointed out that the present brazed CBN wheel has the advantage of wider inter-grit spaces with strong bonding and uniform grit spacing.

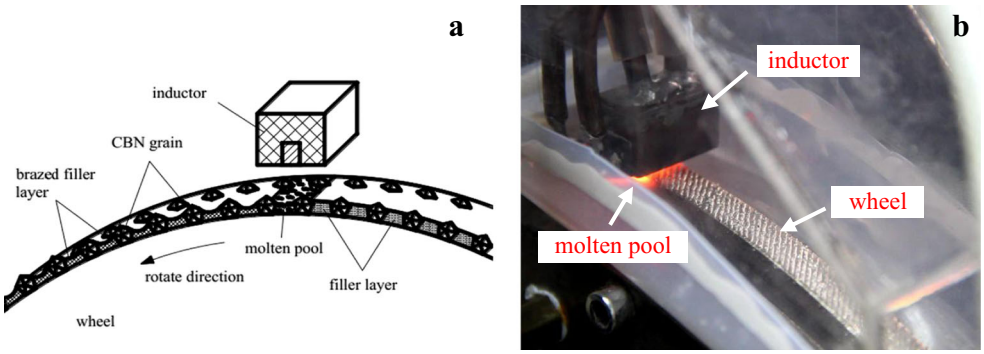

Fig. 1 Illustration of continuous induction brazing of monolayer CBN wheel. **a** Schematic diagram. **b** Brazing setup

However, it should be noticed the fact that the grinding wheel will be exposed in rather high temperature during brazing, and some degree of thermal deformation on the wheel, was inevitable. As a result, the accuracy of the brazed wheel was greatly degraded. This restricted the brazed CBN wheels applying to high-performance grinding, which became the major obstacle of the grinding efficiency and grinding quality improvement. Unfortunately, very few attempts have been involved in this problem so far [7]. Ding et al. [8] developed an assembled monolayer brazed CBN wheel for creep feed grinding of Ti-6Al-4V alloy material. The comparative grinding tests performed with the conventional electroplated and newly developed brazed CBN tools have indicated that highly increased efficiency and prolonged tool lives, as well as low fabrication and use cost, could be achieved by applying the brazed CBN grinding tools. However, since, the brazed CBN wheel in literature [8] was assembled mechanically, and the assemblage errors were inevitable. Moreover, mechanical deformation will occur with the rising of grinding speed. Consequently, assembled brazed wheel was not suitable for high-speed grinding.

Aimed at the challenge of the unexpected wheel deformation after brazing, and solving the urgent and crucial problems of the brazed abrasive grinding wheel mentioned above, a new induction brazing method, named continuous induction brazing, was proposed in this paper. A new monolayer brazed CBN wheel for high-speed grinding was fabricated based on continuous induction brazing technology. A great effort was paid on the interfacial micro-structure and the accuracy of the brazed wheel. Meanwhile, the comprehensive performance of the newly developed CBN wheel was also evaluated in the high-speed grinding tests on Inconel718 superalloy.

Table 1 Experimental conditions

Grinding wheel	Brazed monolayer CBN wheel: grain size 80/100 mesh (150~180 μm), wheel diameter 400 mm; Electroplated monolayer CBN wheel: grain size 80/100 mesh (150~180 μm), wheel diameter 400 mm
Workpiece material	Inconel718 superalloy
Wheel speed v_s (m/s)	80, 100, 120, 150
Workpiece speed v_w (mm/min)	60, 120
Depth of cut a_p (mm)	0.1, 1

2 Theory of induction brazing

Induction brazing is based on electromagnetic induction heating. The heat source of brazing is generated from the induced current in workpiece. Since the heating areas could be precisely controlled and having high heating efficiency, induction brazing has been investigated for several years [9, 10]. During induction heating, the induced current density mainly distributes on the surface alone workpiece thickness (radius), which is called penetration depth (or skin depth) and can be described in millimeters by Eq. 1: [11]

$$\delta = \sqrt{\frac{\rho}{\pi \mu_0 \mu_r f}} (mm) \tag{1}$$

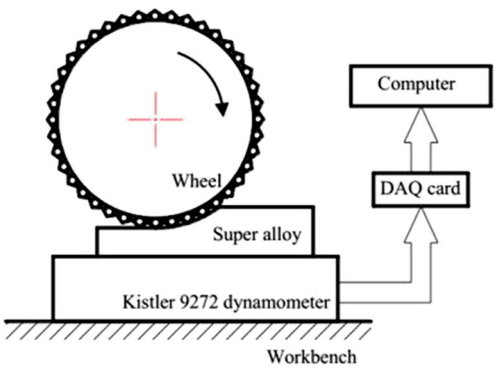

Fig. 2 Schematic of grinding experimental setup

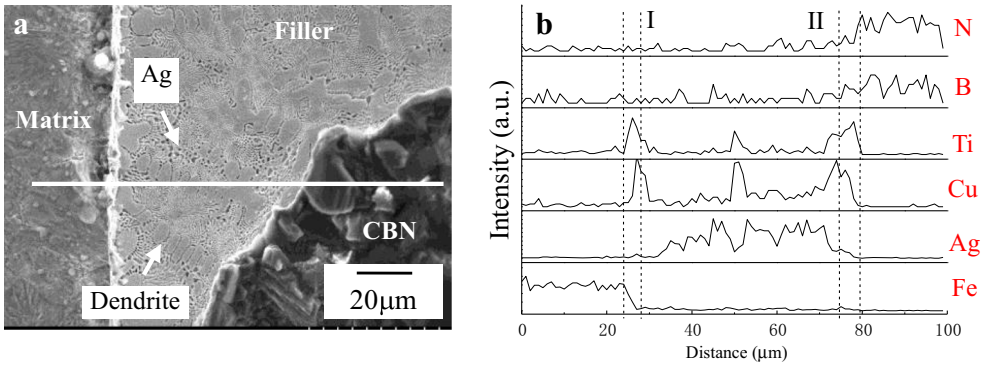

Fig. 3 Cross-section of the brazed joint. **a** SEM image of metallographic structure morphology. **b** Element distribution curves of the joint interface

where δ is the skin depth, ρ is the electrical resistivity of the workpiece, μ_0 is the permeability of vacuum and equals to $4\pi\times10^{-7}$H/m, μ_r is the relative magnetic permeability of the workpiece, and f is the current frequency.

According to Eq. 1, the skin depth is in inverse to the square root of the induction frequency. When applying induction current with ultra-high frequency, such as 1 MHz, the skin depth will greatly reduce. For example, when the current frequency is 1 MHz, the skin depth of ANSI 1045 steel at 900 °C is about 0.55 mm. Generally, approximately 86 % of the electrical power is concentrated in the skin depth of the workpiece. Consequently, the induced heat source concentrates in a very thin surface layer of the workpiece. Former research results have revealed that during ultra-high frequency induction brazing, localized brazing of diamond could be achieved with the width of effective area less than 3 mm [12]. A concentrated heating source in brazing area means that the thermal deformation of the workpiece could decrease remarkably.

3 Experimental procedure

3.1 Fabrication of monolayer brazed CBN wheel

The average size of CBN grain model CBN-230 ranged from 150 to 180 μm, and the active filer was Ag-Cu-Ti alloy powder with melting point 880 °C. The wheel substrate was ANSI 1045 steel with diameter d_s=400 mm and width b= 10 mm. The brazing process was illustrated in Fig. 1. First of all, CBN grains were arranged in a uniform pattern on the periphery of the wheel substrate. A single-pass inductor, which covered with ferrite core and connected to the ultra-high frequency (f=1 MHz) power source, was placed upon the wheel. The gap between the inductor and wheel was 2 mm. During brazing, the wheel counterclockwise rotated, making a relative motion between the inductor and grinding wheel. The speed of such relative motion, which was called scanning speed, was 1 mm/s. The induction power was about 6 kW to ensure that the maximum temperature of the effective area (or molten pool) in brazing procedure was 950 °C. The brazing area was protected under argon atmosphere with a flow rate of 20 L.s^{-1}. As the wheel turning one circle, all the CBN grains were brazed to the wheel substrate (Fig. 1b).

3.2 Grinding setup

The schematic of grinding setup for evaluating the performance of the newly brazed CBN wheel was shown in Fig. 2. The experiment test has been carried out in a surface high-speed grinder (BLOHM). The spindle was capable of running up to 8000 rpm, with maximum power 75 kW. A 5 % solution of a soluble water-based coolant was used as

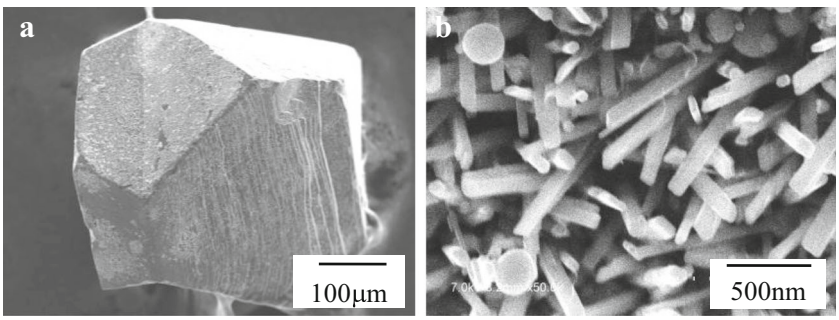

Fig. 4 SEM micrograph of CBN grain and compounds. **a** Brazed grain after etched. **b** Fine compounds around brazed grain

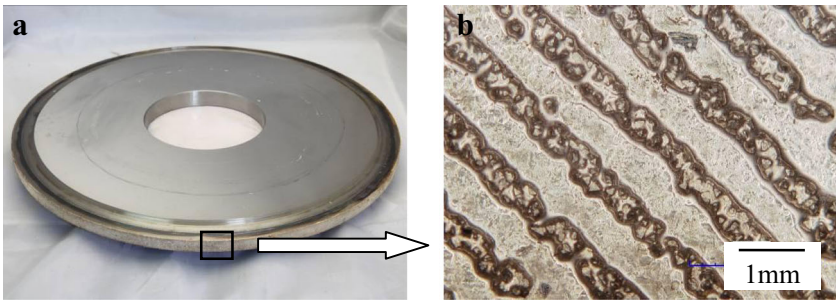

Fig. 5 Surface topography of brazed CBN grinding wheel by continuous induction brazing. **a** Whole macrograph. **b** Grain distribution

the grinding fluid. The workpiece, 80 mm long, 40 mm deep, and 5 mm wide, was held in a fixture which was mounted on Kistler dynamometer (Kistler 9272, Switzerland). Force signals were connected to a data acquisition card, and then recorded by computer system. Ground surface roughness was measured by a Mahr M1 instrument, and measuring direction was vertical to the grinding direction. Micro-morphology of grains and ground surface was observed by a HiroxKH-7700 3D video microscope after cleaning in acetone. The comparative tests were conducted with electroplated CBN wheel for the ground surface quality investigation. Grinding parameters and condition were shown in Table 1.

4 Results and discussions

4.1 Characteristic of brazed CBN grinding wheel

4.1.1 Interfacial micro-structure of CBN grain and filler alloy

The microstructure of CBN grain is examined using a field emission scanning electron microscope (HITACHI S4800), with an energy-dispersive X-ray analyzer (EDX). Figure 3a demonstrates the representative metallographic structure morphology of the joint among matrix, CBN grain, and filler alloy brazed with ultra-high frequency induction. Due to the short processing time in brazing procedure, the small grain α-Ag solid solution and a little dendritic β-Cu in the filler alloy were obtained. The fine and small grain size in the filler is benefit for the strength of the filler layer, comparing to that brazed in vacuum furnace.

Figure 3b illustrates the corresponding element distribution taken by EDX along the white line in Fig. 4a. Preferential segregation of interphases at the filler/matrix interface and filler/grain interface are noted in the joint. The active element Ti of the filler diffuses markedly and gathered in the interfacial of matrix/filler and filler/grain. At interface I (the interface between steel matrix and Ag-Cu-Ti alloy), a titanium-containing intermetallic interlayer, such as Cu, Ti, and Fe, is developed. Interface II (the interface between Ag-Cu-Ti alloy and CBN grain) is enriched in Ti, and also displays a small percentage of Cu, N, and B. The higher Ti concentration in the vicinity of the CBN grain surface implies that Ti from the Ag-Cu-Ti alloy has actually segregated. It can conclude that interfacial reaction has occurred between CBN grain and Ag-Cu-Ti filler.

Figure 4a shows the SEM micro-graph of the brazed CBN grain after electrolysis treatment with vol.10 % HNO_3. Obviously, this corresponds to the chemical reaction at the interface of the filler layer and the CBN grains. Many fine compounds have formed around the brazed grain, as shown in Fig. 5b. Due to the short processing time in continuous induction brazing with ultra-high frequency, the diameter of needle-like compounds is about 100 nm.

Generally speaking, the brazing mechanism of Ag-Cu-Ti filler alloy and CBN grains can be attributed to the preferential migration effect of active element Ti on the surface of grain crystal [13]. Energy-dispersive X-ray analysis results indicate that the compounds in Fig. 4b are composed of N, B, and Ti. The needle-like compounds are confirmed as TiN and TiB2 by X-ray diffraction (XRD) in the former literature [14]. The CBN grains are joined to bonding matrix through chemical reaction among Ti, C, N, and B. The bonding strength is

Table 2 The deformation of the brazed wheel

	Designed value	Before brazing	After brazing	Variation
Bore diameter (mm)	$127_0^{+0.025}$	127.022	127.006	−16
Coaxiality error (μm)	<20	13	19	6
Roundness error (μm)	<20	5	14	9

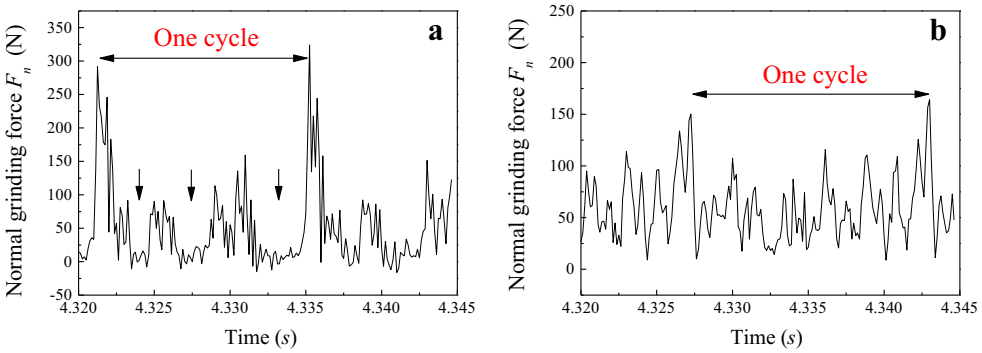

Fig. 6 The original grinding force signals of CBN wheels fabricated by **a** assembling and **b** continuous induction brazing

determined by the amount of the compounds around the grains. During continuous induction brazing, ultra-high frequency alternating magnetic field can induced alternation electromagnetic forces in the molten filler alloy, which is called "induction stirring effect." These alternation electromagnetic forces can speed up the chemical reactions between filler and CBN grains. Consequently, the CBN grain in Fig. 4a is covered with heavy and dense compounds within a short processing time.

4.1.2 Thermal deformation of monolayer brazed CBN grinding wheel

The surface topography of the newly brazed CBN grinding wheel was shown in Fig. 5. It can be seen from Fig. 5b that the CBN grains in the brazed wheel were found to be fairly orderly distributed and well projected above the bonding layer.

The grinding wheel is operating on the high rotating speed when high-speed grinding is conducted. A relatively large roundness and coaxiality error can result in a radial runout on the grinding wheel, leading to an unsatisfactory ground surface quality. During the continuous induction brazing, the rapid heating and cooling may cause phase transformation and thermal plastic deformation in the surface of brazed wheel. The extent of such deformation depends mainly on the temperature history experienced and the instantaneous thermal stress developed. A remarkable deformation can raise roundness and coaxality error. Consequently, in order to investigate the thermal deformation of monolayer brazing CBN wheel in continuous induction brazing with ultra-high frequency, the dimension of the wheel was measured both before and after brazing by coordinate measuring machine (Micro-Hite DCC), and the results were demonstrated in Table 2. As can be seen, the largest deformation was the bore diameter, which was 16 μm after brazing. It should be noted that all the dimensions meet the designed requirements. Finally, the maximum radial runout on the brazed grinding wheel was checked and found to be less than 21 μm.

4.2 Performance of monolayer brazed CBN grinding wheel

4.2.1 Grinding force

Grinding force is one of the most important factors in evaluating the performance of grinding process. Figure 6a showed the segment of original grinding force signal of assembled monolayer brazed CBN wheel for high-speed grinding of Inconel718 superalloy at grinding speed 80 m/s in literature [15]. An obvious periodicity was observed. The double arrow in Fig. 6a indicated one cycle of normal grinding force signal, which was consistent with the grinding speed. Additionally, during one cycle, the grinding force signal violently fluctuated. Occasionally, the signal equaled to 0 which meant no actual grinding depth, and marked in Fig. 6a. This phenomenon revealed the fact that the assembling errors and mechanical deformation of assembled monolayer brazed CBN wheel in high-speed grinding were

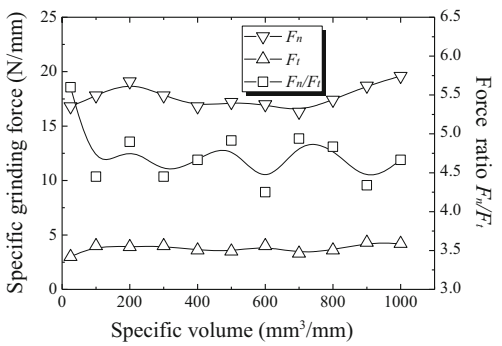

Fig. 7 Variation of specific grinding force with specific volume of material removal under fixed grinding condition

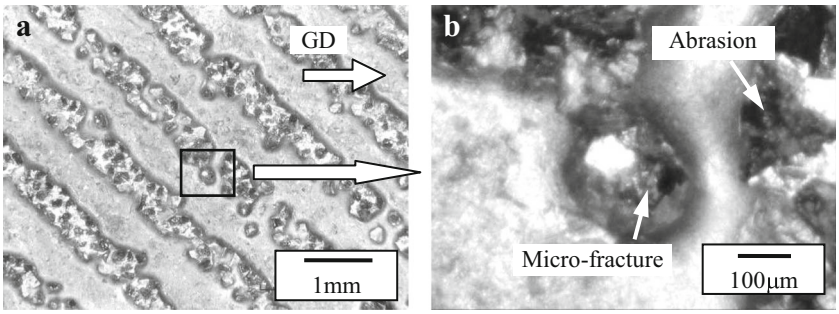

Fig. 8 Wear of brazed CBN wheel. **a** Whole macrograph. **b** Local magnification

both remarkable, and leading a severe runout error on the grinding wheel.

Figure 6b showed the segment of original grinding force signal of monolayer CBN wheel brazed by continuous induction brazing, and the grinding condition was the same as that in Fig. 6a. In spite of one cycle which can be identified in Fig. 6b, it was obvious that the fluctuation of the grinding force signal was much less than that in Fig. 6a. This indicated that the most grains on grinding wheel had a relatively uniform cutting depth during grinding. Small runout error on the grinding wheel by continuous induction brazing played a very essential role in acquiring uniform grinding force signal.

Figure 7 illustrated the variation of specific grinding force with specific volume of material removal under fixed grinding condition of v_s=80 m/s, v_w=120 mm/min, and a_p=0.5 mm. The ratio between normal grinding force F_n and tangential grinding force F_t mainly depended on the machinability of the workpiece material and the sharpness of the grinding wheel, and sharper wheels usually performed lower F_n/F_t. In the present experiments, the specific grinding force and specific volume of material removal were defined as the grinding force and stock material removal divided by the width of the workpiece, respectively. It was obviously from Fig. 7 that both the grinding force components F_t and F_n have not increased much till the specific volume reaching 1000 mm^3/mm. Besides that, the value of the grinding force ratio F_n/F_t was always steady ranging from 4~5.5. This can be attributed to the good bond and sharpness of the brazed CBN wheel.

4.2.2 Wear characteristics

Generally, the grinding performance of a wheel directly depends on the cutting ability of grains on its surface [16]. With regard to cutting ability, all grains with states of whole, abrasion, and micro-fracture can be regarded as strong grains since they still have cutting abilities. Figure 8 displayed the tracing of a sector of the wheel surface after removing specific volume of 1000 mm^3/mm material of Inconel718 superalloy. It can be seen that most of the CBN grains were still on duty in Fig. 8a. No dislodgement of grains has been found even at a relatively adverse grinding condition. In the grinding direction, microfracturing and abrasion of the grains indicated in Fig. 8b were dominant on the wheel surface. This visual observation was consistent with the result in Fig. 7 that the grinding forces were still steady and did not increase with time. Ding et al. [17] pointed out the wear patterns of CBN grains in the brazed abrasive wheels were composed of attrition wear, micro-fracture wear, and grain macro-fracture. The strong joining condition of brazed CBN grains and Ag-Cu-Ti bonding layer played the key role in restraining grain pullout.

4.2.3 Ground surface integrity

Ground surface roughness is one of the significant physical variables that evaluate the accuracy of grinding wheel. Figure 9 showed the ground surface roughness of Inconel718 workpiece under different grinding conditions.

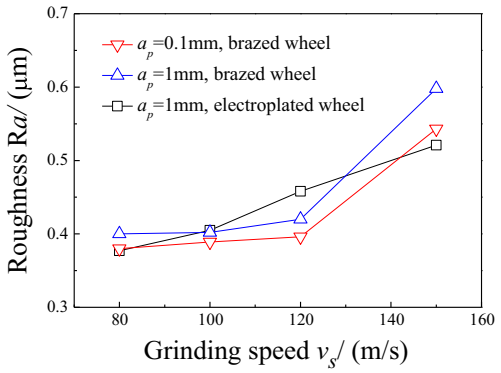

Fig. 9 Ground surface roughness in high-speed grinding of Inconel718 with brazed CBN wheel and electroplated one (v_w=120 mm/min)

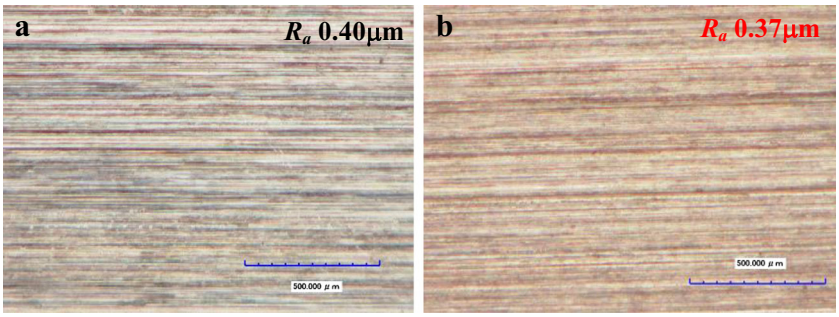

Fig. 10 Ground surface topography of Inconel718 at grinding condition of v_s=80 m/s, v_w=120 mm/min, a_p=1 mm. **a** With brazed CBN wheel. **b** With electroplated CBN wheel

It can be seen that the surface roughness R_a increases slightly when the grinding speed increases from 80 to 150 m/s. While the effects of the grinding depth a_p on surface roughness R_a were not significant. The ground surface roughness with brazed CBN wheel was R_a=0.38 ~0.6 μm in the present study. Moreover, comparative tests were conducted with electroplated wheel under the same grinding parameters as that of the brazed one, and the results were illustrated in Fig. 9. The ground surface roughness R_a was 0.37~0.54 μm with electroplated CBN wheel. In previous research [8], however, ground surface roughness R_a of cast nickel-based superalloy was 1.0 μm. A relatively slight thermal deformation of the brazed wheel is helpful for the low ground surface roughness. Moreover, the uniform protrusion and orderly distribution of the CBN grains on grinding wheel should not be neglected also.

Similar ground surface topographies with brazed CBN wheel and electroplated one were displayed in Fig. 10. With the same grinding parameters, the ground surface roughness R_a were 0.4 and 0.37 μm. The micro-grooves and cutting trace, which were natural scratches produced by the interaction of CBN grains with work material, were observed at all the ground surfaces. No obvious tearing surface and cracks were found. It meant that two types of CBN wheels had the similar ground surface quality in the high-speed grinding of Inconel718 superalloy.

The micro-hardness was measured using the Vickers method with $HV_{0.1}$ of the ground sub-surface in Fig. 11. The black arrow in Fig. 11a indicated the ground surface. Especially, the measurement of the hardness was conducted at every 10 up to 250 μm below the ground surface. The results in terms of hardness fluctuating with the distance from ground surface were plotted in Fig. 11b. A grinding of the soften layer with the depth about 20 μm near ground surface can be observed. The minimum hardness value was 420 $HV_{0.1}$, which was around 7 % lower than the bulk material value of 450 $HV_{0.1}$. Such soften layer was mainly produced by the rising of grinding temperature in the grinding contact area. A 7 % soften degree indicated the grinding temperature was no more than 200 °C in comparison with the results in literature [18, 19].

The optical metallurgical image of the ground Inconel718 superalloy was showed in Fig. 12. No micro-crack and white layer were observed. Additionally, the plastic deformation of lattice on ground surface was not obvious, and the depth of the plastic deformation layer was around 10 μm.

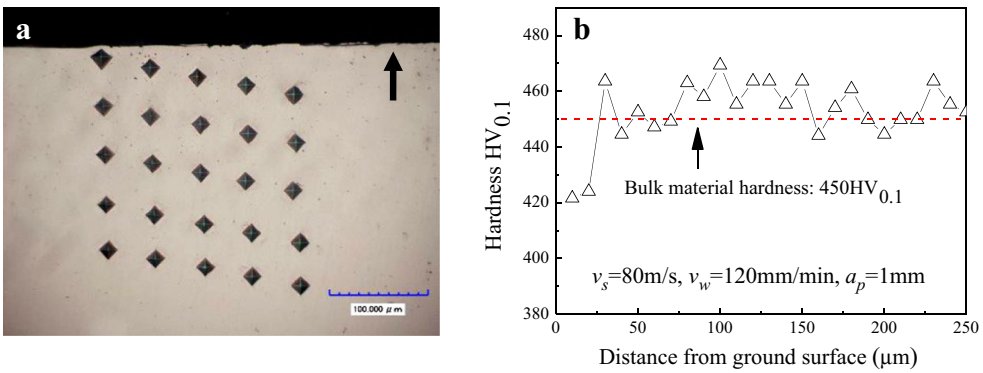

Fig. 11 Hardness distribution on the ground sub-surface **a** Measure points. **b** Hardness distribution

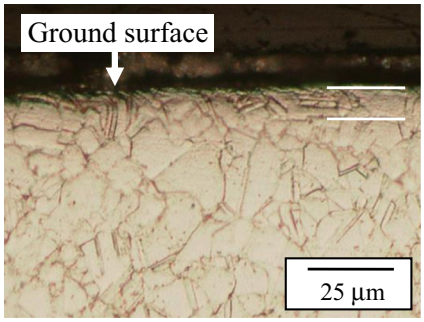

Fig. 12 Metallurgical morphology of ground sub-surface

5 Conclusions

Aimed at the challenge of the unexpected wheel deformation after brazing, a monolayer brazed CBN wheel for high-speed grinding has been fabricated based on continuous induction brazing technology successfully. The interfacial micro-structure, accuracy, and the comprehensive performance of the newly developed CBN wheel have been investigated. The creative conclusions can be drawn based on the experiment results:

1. The continuous induction brazing with scanning-speed 1 mm/s is chosen for fabrication of CBN grinding wheel. The interfacial reaction has occurred between the interfacial of matrix/filler and filler/grain respectively. Depending on the chemical compounds around the brazed CBN grains, the CBN grains are joined to wheel substrate firmly.
2. The accuracy of brazed wheel meets the designed requirements. The maximum thermal deformation of the brazed wheel is less than 16 μm. And the maximum radial runout on the brazed grinding wheel is found to be less than 21 μm.
3. High-speed performance of brazed CBN grinding wheel for the grinding of Inconel718 superalloy shows that the grinding wheel has good bonding strength. The ground surface of superalloy is free of crack, and the surface roughness R_a is 0.38~0.6 μm.

Acknowledgments The authors would like to gratefully acknowledge the financial support of this research by the National Natural Science Foundation of China (No. 51275231) and Natural Science Foundation of the Higher Education Institutions of Jiangsu Province, China (No. 14KJB460011).

References

1. Qu NS, Xu ZY (2013) Improving machining accuracy of electrochemical machining blade by optimization of cathode feeding directions. Int J Adv Manuf Technol 68(5-8):1565–1572
2. Webster J, Tricard M (2004) Innovations in abrasive products for precision grinding. CIRP Ann Manuf Technol 53(2):597–617
3. Soo SL, Hood R, Lannette M, Aspinwall DK, Voice WE (2011) Creep feed grinding of burn-resistant titanium (BuRTi) using superabrasive wheels. Int J Adv Manuf Technol 53(9-12):1019–1026
4. Chattopadhyay AK, Hintermann HE (1993) On brazing of cubic boron nitride abrasive crystals to steel substrate with alloys containing Cr or Ti. J Mater Sci 28(21):5887–5893
5. Bhaduri D, Kumar R, Chattopadhyay AK (2011) On the grindability of low-carbon steel under dry, cryogenic and neat oil environments with monolayer brazed cBN and alumina wheels. Int J Adv Manuf Technol 57(9-12):927–943
6. Pal B, Chattopadhyay AK, Chattopadhyay AB (2010) Development and performance evaluation of monolayer brazed cBN grinding wheel on bearing steel. Int J Adv Manuf Technol 48(9-12):935–944
7. Zhan YJ, Xu XP (2012) An experimental investigation of temperatures and energy partition in grinding of cemented carbide with a brazed diamond wheel. Int J Adv Manuf Technol 61(1-4):117–125
8. Ding WF, Xu JH, Chen ZZ, Su HH, Fu YC (2010) Grindability and surface integrity of cast nickel-based superalloy in creep feed grinding with brazed CBN abrasive wheels. Chin J Aeronaut 23(04): 501–510
9. Chattopadhyay AK, Chollet L, Hintermann HE (1991) Induction brazing of diamond with Ni-Cr hardfacing alloy under argon atmosphere. Surf Coat Technol 45(1-3):293–298
10. Li QL, Xu JH, Su HH (2013) Simulation of temperature field in ultra-high frequency induction heating and verification. Trans Nanjing Univ Aeronaut Astronaut 30(2):155–161
11. Valery R, Don L, Raymond C, Micah B (2003) Handbook of induction heating. Marcel Dekker Inc, New York
12. Su HH, Li QL, Xu JH, Fu YC (2012) Study on influence factors of temperature in localized ultra-high frequency induction brazing. Trans Chin Weld Inst 33(12):13–17
13. Johari MR, Hadian AM (2014) Effect of brazing time on microstructure and mechanical properties of cubic boron nitride/steel joints. Ceram Int 40(6):8519–8524
14. Ding WF, Xu JH, Shen M, Fu YC, Xiao B (2006) Thermodynamic and kinetic analysis of interfacial reaction between CBN and titanium activated Ag-Cu alloy. Mater Sci Technol 22(1):105–109
15. Xu P (2011) High speed grinding of nickel superalloy using CBN wheels. Master dissertation, Nanjing, China
16. Malkin S (1989) Grinding technology: theory and application of machining with abrasives. John Wiley & Sons, New York
17. Ding WF, Xu JH, Chen ZZ, Su HH, Fu YC (2010) Wear behavior and mechanism of single-layer brazed CBN abrasive wheels during creep-feed grinding cast nickel-based superalloy. Int J Adv Manuf Technol 51(5-8):541–550
18. Yao CF, Jin QC, Huang XC, Wu DX, Ren JX, Zhang DH (2013) Research on surface integrity of grinding Inconel 718. Int J Adv Manuf Technol 65(5-8):1019–1030
19. Chen ZZ, Xu JH, Ding WF, Ma CY, Fu YC (2015) Grinding temperature during high-efficiency grinding Inconel 718 using porous CBN wheel with multilayer defined grain distribution. Int J Adv Manuf Technol 77(1-4):165–172